Journal of AppliedMath 2025, 3(1), 1986.
https://doi.org/10.59400/jam1986

Article

Fatigue damage model of neoprene rubber sandwiched with bi-directional carbon fabric

Krishna Nair[1], Shrutva Chavda[2], Pooja Choudhary[2], Pinkal Patel[1], Anil Chavada[2], Jashvant D. Rathod[1], Rajesh C. Shah[2,*]

[1] Department of Applied Mechanics & Structural Engineering, Faculty of Technology & Engineering, The Maharaja Sayajirao University of Baroda, Vadodara 390001, India
[2] Department of Applied Mathematics, Faculty of Technology & Engineering, The Maharaja Sayajirao University of Baroda, Vadodara 390001, India
*** Corresponding author:** Rajesh C. Shah, dr_rcshah@yahoo.com

CITATION

Nair K, Chavda S, Choudhary P, et al. Fatigue damage model of neoprene rubber sandwiched with bi-directional carbon fabric. Journal of AppliedMath. 2025; 3(1): 1986. https://doi.org/10.59400/jam1986

ARTICLE INFO

Received:5 November 2024
Accepted: 21 January2025
Available online: 19 February 2025

Abstract: Fatigue is a phenomenon that occurs in materials when they are subjected to repetitive or cyclic loading, which can lead to the accumulation of damage over a time. The purpose of the present study is to develop a fatigue damage model incorporating experimental test results of axial tension and fatigue that utilizes the principles of continuum damage mechanics (CDM) to predict the damage accumulation in composite. Experimental testing in axial tensile tests involves dumbbell specimens of neoprene rubber sandwiched with bi-directional carbon fabric to constitute a composite material with the help of which material constants C_{10}, C_{20}, and C_{30} parameters are evaluated by the curve-fitting method. Fatigue tests were conducted for different displacements, from which constants s_0 and S_0 were figured out using a linear regression method. A mathematical model is developed, and MATLAB is used to relate stress and strain in Yeoh's strain energy function to describe the nonlinear elastic behavior of elastomers incorporating material parameters evaluated by axial tensile tests and fatigue tests. The MATLAB script was run in ANSYS with this modified Yeoh hyperelastic model for evaluation of damage in composite and compared with damage evaluated by image processing software in scanning electron microscope (SEM) images for validation purposes.

Keywords: fatigue; CDM; mathematical modelling; elastomer; rubber; hyperelastic model; strain energy function

1. Introduction

Rubber's unique combination of properties makes it indispensable in various industries. Also, its ability to resist substantial deformation without permanent changes and its elasticity make it a go-to material for many applications. But one of the main challenges with rubber components is fatigue failure due to cyclic loading. Many researchers and engineers employ various methods to experiment and to model for predicting fatigue life, considering various factors such as materials stress-strain behavior, environmental conditions, multi-axial loading conditions, specific geometry, and design of components [1,2]. Experimental data incorporated in finite element analysis (FEA) is another valuable tool for predicting the fatigue life of rubber components. Advancements in material science and computational modeling continue to improve the understanding of rubber fatigue and enhance the ability to predict component performance accurately [3,4].

On the other side, degradation occurs due to the repetitive applications of stress and strain, which leads to the initiation and propagation of defects within the material.

The continuum damage mechanics (CDM) approach is indeed a valuable framework for understanding and predicting the fatigue damage more accurately in rubber-like materials. Initiation and accumulation of damage evaluation in tested samples with the help of microscopy can be employed to validate CDM predictions [5–7]. These damages can include microcracks, voids, or other forms of degradation. Over a time, these individual damages can coalesce or propagate, leading to the formation of macroscopic cracks until the material produces local or overall fractures [8]. An analytical approach was also used to determine the mechanical properties of laminated composites by progressive damage analysis using ANSYS [9].

Shangguan [10] proposed different fatigue life prediction models using experimental damage parameters to predict the fatigue life of natural rubber using dumbbell cylindrical kinds of specimens. In [11], Shangguan et al. explored the relationship between the tensile fatigue life of rubber specimens with three different shapes and various damage parameters as well as the effect of the shapes on the fatigue life prediction model. Gehrmann et al. [12] proposed to convert strain variations into constant equivalent strains fitting the curve, where finite element simulation indicated that this approach can also be applied to specimens with other geometries. Tensile strain test-based experimental data of 30 positive and negative *R*-ratios were used to predict fatigue life in [13,14]. Li et al. [15] studied combined physical tests on material and finite element analysis to predict the fatigue life using maximum principal strains as the fatigue criteria. Papadopoulos et al. [16] suggest a mathematical equation to describe fatigue crack growth rate in natural rubber and styrene–butadiene rubber. Ayoub et al. [17] put forward a fatigue criterion-based CDM theory to predict the fatigue life of rubber. Experiments were performed to determine the mechanical properties of composites and the effect of fiber orientation in bi-directional laminates.

Many other researchers also investigated various mechanical properties like crack growth, fatigue life and proposed mathematical models based on CDM on natural and reinforced rubber [18,19]. Parmar et al. [20] investigated the mechanical properties of bi-directional carbon fiber composite materials. All these investigations were carried out on natural and reinforced rubber materials; however, neoprene rubber needs special attention for its mechanical properties and fatigue life. Further, inherent limitations of rubber material demand additional strengthening material in the form of reinforcement to make it the most advanced composite to overcome the weakness of rubber material. Neoprene rubber sandwiched with carbon fabric resolves many challenging issues in current applications but has not been paid sufficient attention. Comprehensive work of derivation of parameters from experiment, fatigue simulation, and damage evaluation of the composite has also not been done yet.

The present study aims at conducting uniaxial tensile static and fatigue testing of dumbbell composite (neoprene rubber sandwiched with bi-directional carbon fabric) specimens for derivation of parameters for use in MATLAB script and running this MATLAB script in the existing Yeoh model in ANSYS to predict fatigue life. This novel approach utilizes available resources of simple experimental facilities and the existing Yeoh model in ANSYS to predict the fatigue life of the composite, which eliminates many complex processes. The damage evaluation adopting the CDM approach is also validated by SEM images of tested samples.

2. Curve-fitting of Yeoh model

Standard tests have been established to assess the stress-strain behavior of rubber under simple stress conditions [21,22]. Among these, the uniaxial tension test stands out as one of the most popular and widely utilized due to its straightforward nature. ANSYS offers curve-fitting tools that enable the derivation of material constants for hyperelastic models from characterization data [9]. This data can be inputted into the FEA software in the form of tab-delimited stress-strain text files derived from manipulated characterization data for the uniaxial tension test. The coefficients within the strain energy functions can be interpreted as material constants.

3. Modeling using continuum damage mechanics

The Yeoh model is used as a hyperelastic material model that is suitable for modeling the behavior of isotropic, incompressible, rubber-like materials because of its wide application and simple expression [2,4]. The Yeoh model is the best for various kinds of deformations but may not be appropriate for applications involving very large or very small deformations. Modification is necessary to accurately predict material behavior under such special conditions wherein rubber materials undergo little damage and much fatigue resistance because of being reinforced with bi-directional carbon fabric. Modification in the Yeoh model through changes in the constitutive equation of damage with respect to a number of cycles ensures that it accurately reflects the fatigue properties of the newly introduced composite, enhancing its reliability in practical applications. This model is beneficial for describing the nonlinear stress-strain relationship exhibited by such materials that undergo various deformations.

In this section, the Yeoh model is reformulated by incorporating parameters evaluated from the uniaxial nominal stress-strain relation and fatigue test for computation of the damage strain energy release rate in elastomers. Thus, the modified Yeoh model provides the damage of the elastomeric composites with respect to the number of cycles under fatigue loading.

3.1. Modified theoretical model

The relation of the Yeoh strain energy potential is given by

$$W = C_{10}(I_1 - 3) + C_{20}(I_1 - 3)^2 + C_{30}(I_1 - 3)^3, \tag{1}$$

where C_{10}, C_{20}, C_{30} are material parameters determined by the experimental nominal stress–strain relation, and I_1 is an invariant of the Green deformation tensor and is given by

$$I_1 = \lambda_1^2 + \lambda_2^2 + \lambda_3^2 \tag{2}$$

in which $\lambda_1, \lambda_2, \lambda_3$ are the principal extension ratios, and for uniaxial stress state.

$$\lambda_1 = \lambda, \lambda_2 = \lambda_3 = \frac{1}{\sqrt{\lambda}}, \tag{3}$$

where λ is the stretch in the loading direction. Referring to [18], the nominal strain in the loading direction is given by

$$\varepsilon = \lambda - 1 \tag{4}$$

To determine the uniaxial nominal normal stress T_W , we consider the principle of virtual work in the form.

$$T_W = \frac{\partial W}{\partial \lambda} \tag{5}$$

Using Equations (2) and (3) in Equation (1) yields *W* for the uniaxial stress state form as

$$W = C_{10}\left(\lambda^2 + \frac{2}{\lambda} - 3\right) + C_{20}\left(\lambda^2 + \frac{2}{\lambda} - 3\right)^2 + C_{30}\left(\lambda^2 + \frac{2}{\lambda} - 3\right)^3. \tag{6}$$

Using Equations (5) and (6), the nominal stress and strain relation under uniaxial tension is expressed as

$$T_W = \frac{\partial W}{\partial \lambda} = C_{10}\left(2\lambda - \frac{2}{\lambda^2}\right) + 2C_{20}\left(\lambda^2 + \frac{2}{\lambda} - 3\right)\left(2\lambda - \frac{2}{\lambda^2}\right) + 3C_{30}\left(\lambda^2 + \frac{2}{\lambda} - 3\right)^2\left(2\lambda - \frac{2}{\lambda^2}\right). \tag{7}$$

Based on the CDM theory [19], the effective nominal normal stress is expressed as

$$\bar{T}_W = \frac{T_W}{1 - D} \tag{8}$$

therefore, the nominal stress–strain relation of a damaged material is the same in form as that of an undamaged material in Equation (7), which becomes.

$$\bar{T}_W = \frac{T_W}{1 - D} = C_{10}\left(2\lambda - \frac{2}{\lambda^2}\right) + 2C_{20}\left(\lambda^2 + \frac{2}{\lambda} - 3\right)\left(2\lambda - \frac{2}{\lambda^2}\right) + 3C_{30}\left(\lambda^2 + \frac{2}{\lambda} - 3\right)^2\left(2\lambda - \frac{2}{\lambda^2}\right) \tag{9}$$

where *D* is a damage variable.

Again, based on the CDM theory, within the hypothesis of isotropic damage, the constitutive equation for damage evolution is given by

$$\dot{D} = -\frac{\partial \phi^*}{\partial y} \tag{10}$$

where φ^* is the dissipation potential and *y* is the damage strain energy release rate.

Lemaitre [19] assumed the potential of dissipation as

$$\phi^* = \frac{S_0}{s_0 + 1}\left(\frac{-y}{S_0}\right)^{s_0 + 1} \tag{11}$$

where s_0 and S_0 are material parameters.

Referring to [7], the strain energy of a damaged material is also in the same form as that of an undamaged material. But the damage strain energy should be a function of the effective nominal normal stress. Therefore, in the uniaxial stress state, the damage strain energy release rate *y* is defined as

$$-y = \frac{\partial W}{\partial D} = \frac{\partial W(\bar{T}_W)}{\partial D} \tag{12}$$

Using Equations (7), Equation (12) becomes.

$$-y=\left[C_{10}\left(2\lambda-\frac{2}{\lambda^2}\right)+2C_{20}\left(\lambda^2+\frac{2}{\lambda}-3\right)\left(2\lambda-\frac{2}{\lambda^2}\right)+3C_{30}\left(\lambda^2+\frac{2}{\lambda}-3\right)^2\left(2\lambda-\frac{2}{\lambda^2}\right)\right]\frac{\partial\lambda(\bar{T}_W)}{\partial D}. \tag{13}$$

Taking the partial derivative of Equation (9) with respect to *D*, we have

$$\frac{\partial\lambda(\bar{T}_W)}{\partial D}=\frac{T_W}{(1-D)^2}\frac{1}{\begin{bmatrix}C_{10}\left(2+\frac{4}{\lambda^3}\right)+2C_{20}\left\{\left(2\lambda-\frac{2}{\lambda^2}\right)^2+\left(\lambda^2+\frac{2}{\lambda}-3\right)\left(2+\frac{4}{\lambda^3}\right)\right\}\\+3C_{30}\left\{2\left(\lambda^2+\frac{2}{\lambda}-3\right)\left(2\lambda-\frac{2}{\lambda^2}\right)^2+\left(\lambda^2+\frac{2}{\lambda}-3\right)^2\left(2+\frac{4}{\lambda^3}\right)\right\}\end{bmatrix}}. \tag{14}$$

Substituting Equation (14) into Equation (13) and using Equation (9), the damage strain energy release rate is

$$-y=\frac{1}{1-D}\left[C_{10}\left(2\lambda-\frac{2}{\lambda^2}\right)+2C_{20}\left(\lambda^2+\frac{2}{\lambda}-3\right)\left(2\lambda-\frac{2}{\lambda^2}\right)+3C_{30}\left(\lambda^2+\frac{2}{\lambda}-3\right)^2\left(2\lambda-\frac{2}{\lambda^2}\right)\right]^2$$
$$\times\frac{1}{\begin{bmatrix}C_{10}\left(2+\frac{4}{\lambda^3}\right)+2C_{20}\left\{\left(2\lambda-\frac{2}{\lambda^2}\right)^2+\left(\lambda^2+\frac{2}{\lambda}-3\right)\left(2+\frac{4}{\lambda^3}\right)\right\}\\+3C_{30}\left\{2\left(\lambda^2+\frac{2}{\lambda}-3\right)\left(2\lambda-\frac{2}{\lambda^2}\right)^2+\left(\lambda^2+\frac{2}{\lambda}-3\right)^2\left(2+\frac{4}{\lambda^3}\right)\right\}\end{bmatrix}}. \tag{15}$$

Using Equations (10) and (11),

$$\dot{D}=-\frac{\partial}{\partial y}\left[\frac{S_0}{s_0+1}\left(\frac{-y}{S_0}\right)^{s_0+1}\right]=-\left[\frac{S_0}{s_0+1}(s_0+1)\left(\frac{-y}{S_0}\right)^{s_0}\left(\frac{-1}{S_0}\right)\right]=\left(\frac{-y}{S_0}\right)^{s_0}. \tag{16}$$

Under a cyclic loading condition, the damage will accumulate with the number of cycles and the damage evolution will depend on the strain amplitude. In this case, $\dot{D}=\frac{dD}{dN}$, where *N* is the number of cycles. The fatigue damage evolution per cycle is then expressed using Equations (15) and (16) as

$$\frac{dD}{dN}=\begin{bmatrix}\frac{1}{S_0(1-D)}\left\{C_{10}\left(2\lambda-\frac{2}{\lambda^2}\right)+2C_{20}\left(\lambda^2+\frac{2}{\lambda}-3\right)\left(2\lambda-\frac{2}{\lambda^2}\right)+3C_{30}\left(\lambda^2+\frac{2}{\lambda}-3\right)^2\left(2\lambda-\frac{2}{\lambda^2}\right)\right\}^2\times\\\begin{bmatrix}C_{10}\left(2+\frac{4}{\lambda^3}\right)+2C_{20}\left\{\left(2\lambda-\frac{2}{\lambda^2}\right)^2+\left(\lambda^2+\frac{2}{\lambda}-3\right)\left(2+\frac{4}{\lambda^3}\right)\right\}\\+3C_{30}\left\{2\left(\lambda^2+\frac{2}{\lambda}-3\right)\left(2\lambda-\frac{2}{\lambda^2}\right)^2+\left(\lambda^2+\frac{2}{\lambda}-3\right)^2\left(2+\frac{4}{\lambda^3}\right)\right\}\end{bmatrix}^{-1}\end{bmatrix}^{s_0}. \tag{17}$$

Assuming that the damage variable *D* is zero at the beginning of the cyclic loading, that is, $D=0$ when $N=0$, then the damage value at any cycle can be determined by integrating Equation (17), therefore

$$\int_0^D (1-D)^{s_0} dD = \int_0^N \left[\begin{array}{l} \frac{1}{S_0}\left\{C_{10}\left(2\lambda-\frac{2}{\lambda^2}\right)+2C_{20}\left(\lambda^2+\frac{2}{\lambda}-3\right)\left(2\lambda-\frac{2}{\lambda^2}\right)+3C_{30}\left(\lambda^2+\frac{2}{\lambda}-3\right)^2\left(2\lambda-\frac{2}{\lambda^2}\right)\right\}^2 \times \\ \left[\begin{array}{l} C_{10}\left(2+\frac{4}{\lambda^3}\right)+2C_{20}\left\{\left(2\lambda-\frac{2}{\lambda^2}\right)^2+\left(\lambda^2+\frac{2}{\lambda}-3\right)\left(2+\frac{4}{\lambda^3}\right)\right\} \\ +3C_{30}\left\{2\left(\lambda^2+\frac{2}{\lambda}-3\right)\left(2\lambda-\frac{2}{\lambda^2}\right)^2+\left(\lambda^2+\frac{2}{\lambda}-3\right)^2\left(2+\frac{4}{\lambda^3}\right)\right\} \end{array} \right]^{-1} \end{array} \right]^{s_0} dN. \quad (18)$$

As

$$(1-D)^{s_0} dD = \frac{d[1-(1-D)^{s_0+1}]}{s_0+1},$$

Equation (18) becomes

$$\int_0^D \frac{d[1-(1-D)^{s_0+1}]}{s_0+1} = \int_0^N \left[\begin{array}{l} \frac{1}{S_0}\left\{C_{10}\left(2\lambda-\frac{2}{\lambda^2}\right)+2C_{20}\left(\lambda^2+\frac{2}{\lambda}-3\right)\left(2\lambda-\frac{2}{\lambda^2}\right)+3C_{30}\left(\lambda^2+\frac{2}{\lambda}-3\right)^2\left(2\lambda-\frac{2}{\lambda^2}\right)\right\}^2 \times \\ \left[\begin{array}{l} C_{10}\left(2+\frac{4}{\lambda^3}\right)+2C_{20}\left\{\left(2\lambda-\frac{2}{\lambda^2}\right)^2+\left(\lambda^2+\frac{2}{\lambda}-3\right)\left(2+\frac{4}{\lambda^3}\right)\right\} \\ +3C_{30}\left\{2\left(\lambda^2+\frac{2}{\lambda}-3\right)\left(2\lambda-\frac{2}{\lambda^2}\right)^2+\left(\lambda^2+\frac{2}{\lambda}-3\right)^2\left(2+\frac{4}{\lambda^3}\right)\right\} \end{array} \right]^{-1} \end{array} \right]^{s_0} dN \quad (19)$$

Thus, the relation between the damage variable *D* and the number of cycles *N* is given by

$$D = 1 - \left[1 - (s_0 + 1) \times \left[\begin{array}{l} \frac{1}{S_0}\left\{C_{10}\left(2\lambda-\frac{2}{\lambda^2}\right)+2C_{20}\left(\lambda^2+\frac{2}{\lambda}-3\right)\left(2\lambda-\frac{2}{\lambda^2}\right)+3C_{30}\left(\lambda^2+\frac{2}{\lambda}-3\right)^2\left(2\lambda-\frac{2}{\lambda^2}\right)\right\}^2 \times \\ \left[\begin{array}{l} C_{10}\left(2+\frac{4}{\lambda^3}\right)+2C_{20}\left\{\left(2\lambda-\frac{2}{\lambda^2}\right)^2+\left(\lambda^2+\frac{2}{\lambda}-3\right)\left(2+\frac{4}{\lambda^3}\right)\right\} \\ +3C_{30}\left\{2\left(\lambda^2+\frac{2}{\lambda}-3\right)\left(2\lambda-\frac{2}{\lambda^2}\right)^2+\left(\lambda^2+\frac{2}{\lambda}-3\right)^2\left(2+\frac{4}{\lambda^3}\right)\right\} \end{array} \right]^{-1} \end{array} \right]^{s_0} N \right]^{\frac{1}{(s_0+1)}} \quad (20)$$

here, s_0 and S_0 are referred to as goodness of fit and are determined by experimental fatigue tests as a function of the nominal strain amplitude. MATLAB script is written to modify the model and run it in ANSYS for damage analysis of the elastomeric composite incorporating test results C_{10}, C_{20} and C_{30} from the axial tensile test, and s_0 and S_0 from the fatigue test.

3.2. Experimental procedure: Material and specimen preparation

The elastomer composite used is neoprene rubber sandwiched with bi-directional carbon fabric as shown in **Figure 1**. Two layers of neoprene rubber and one layer of carbon fabric in the composite specimen are used for testing. The standard die was used to cut the specimen of the composite for specified dimensions according to ASTMD 412-16 as shown in **Figure 2**. The layers in the composites are adhered by cyanoacrylate glue. The glue is applied on a single side of two neoprene rubber sheets and one piece of carbon fabric in between them. The specimen was kept under a constant load (weight) for 24 h for proper bonding. This specimen was tested under static uniaxial tension and fatigue loading.

Figure 1. Neoprene rubber sandwiched with a bi-directional carbon fabric composite specimen.

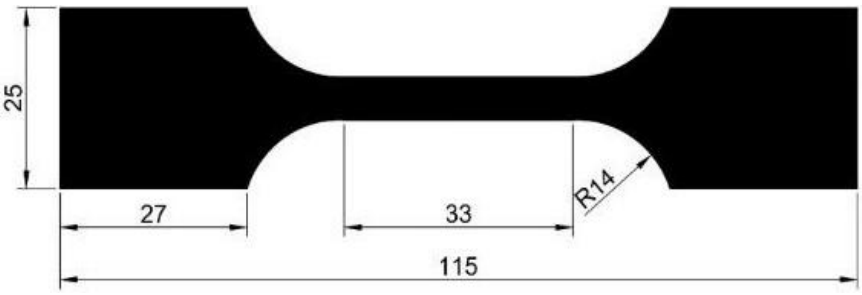

Figure 2. Standard die for cutting dumbbell specimen.

3.2.1. Static uniaxial tensile test

The elastomeric composite utilized in the present investigation is found to conform well to the existing Yeoh model in ANSYS (also called the third-order reduced polynomial form) as shown in **Figure 3**, which is deemed to be an appropriate fit. To determine C_{10}, C_{20} and C_{30} experimentally for neoprene rubber sandwiched with carbon fabric laminate, a static uniaxial tension test was performed on the composite to get strains and stresses of the material and eventually measure the resulting force or displacements. These tests provide data that can be fitted to the existing Yeoh model in ANSYS to extract the material constants. Subsequently, material constants (C_{10}, C_{20}, C_{30}) as given in **Table 1** are determined for this composite using the existing Yeoh model, which are then utilized in the modification of the Yeoh model for fatigue analysis purposes.

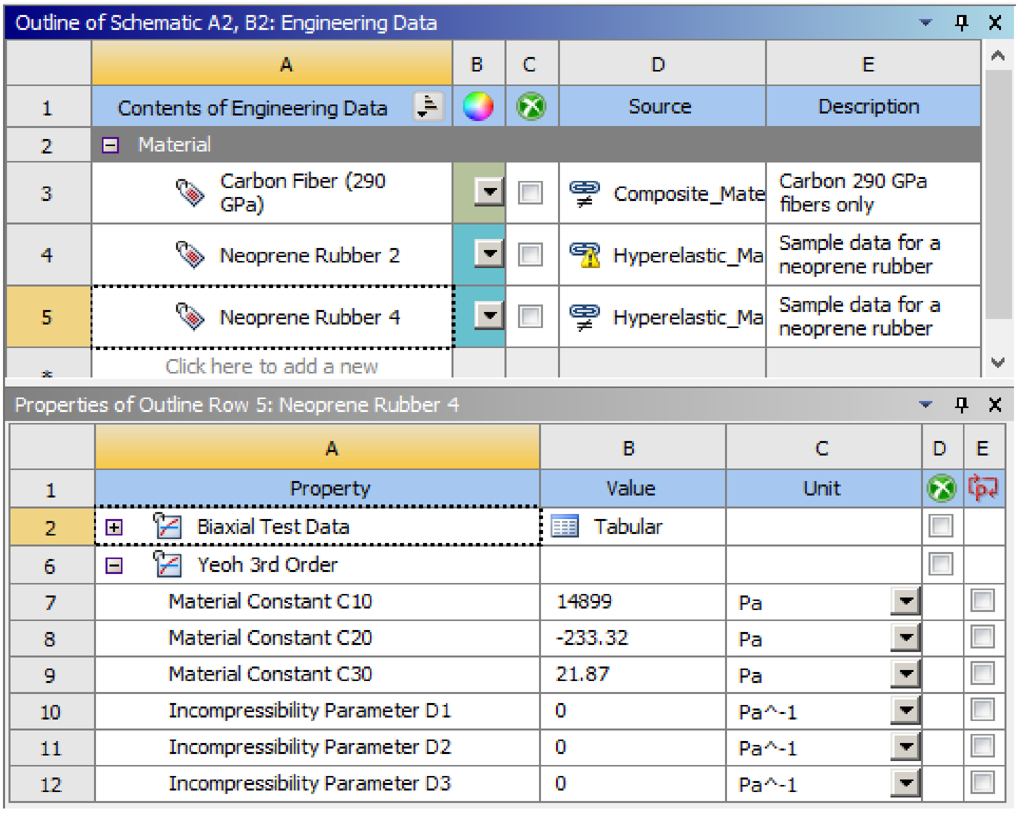

Outline of Schematic A2, B2: Engineering Data

	A	B	C	D	E
1	Contents of Engineering Data			Source	Description
2	Material				
3	Carbon Fiber (290 GPa)			Composite_Mate	Carbon 290 GPa fibers only
4	Neoprene Rubber 2			Hyperelastic_Ma	Sample data for a neoprene rubber
5	Neoprene Rubber 4			Hyperelastic_Ma	Sample data for a neoprene rubber
*	Click here to add a new				

Properties of Outline Row 5: Neoprene Rubber 4

	A	B	C	D	E
1	Property	Value	Unit		
2	Biaxial Test Data	Tabular			
6	Yeoh 3rd Order				
7	Material Constant C10	14899	Pa		
8	Material Constant C20	-233.32	Pa		
9	Material Constant C30	21.87	Pa		
10	Incompressibility Parameter D1	0	Pa^-1		
11	Incompressibility Parameter D2	0	Pa^-1		
12	Incompressibility Parameter D3	0	Pa^-1		

(a)

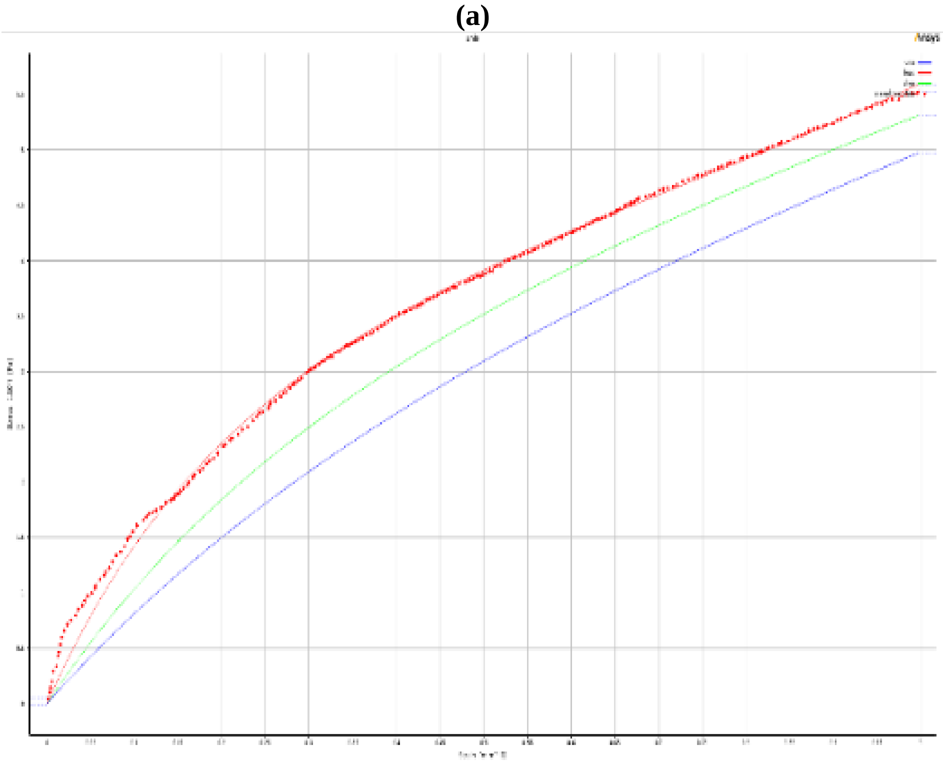

(b)

Figure 3. Curve fitting of Yeoh model in ANSYS **(a)** Values of material properties; **(b)** Curve-fitting of **(a)**.

Table 1. Materials parameters obtained from curve-fitting in ANSYS.

Material Parameters	Values
C_{10}	14899
C_{20}	–233.32
C_{30}	21.87

3.2.2. Fatigue test

The samples are loaded into a tension-tension fatigue endurance test on MTS, which is subjected to repeated stresses under a constant strain rate. ASTM D3039 for tensile testing [21] and ASTM D412 for rubber (Black, Gray) [22] are referred to for this experimental testing. Both of these standards are widely recognized in the industry for ensuring consistency and accuracy in materials testing.

A fatigue testing setup of an MTS series 312 servo-hydraulic machine with a 10T capacity shown in **Figure 4** has been used for the study. A large number of tests had been conducted to determine the fatigue life of the specimens experimentally at the frequency of 3Hz at room temperature. The stress ratio R is controlled to $R = 0$ ($R = \sigma_{\mathrm{min}/}\, \sigma_{\mathrm{max}}$) using sinusoidal waveform control. The number of cycles 100, 1000 and 10,000 are assigned as loading sequences for fatigue testing based on the plot required for the composite life prediction. The test is conducted under displacement control. Strain indicator is used for the strain measurement.

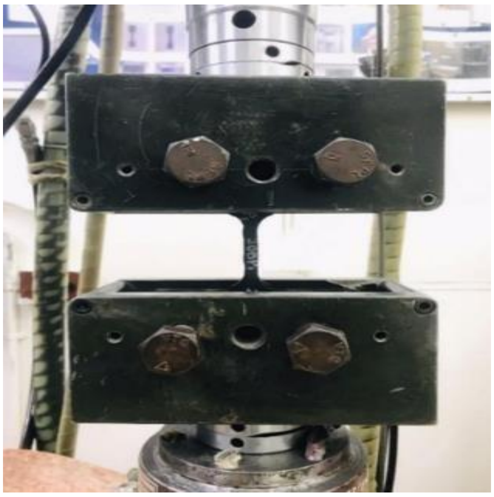

Figure 4. The rubber specimen is being tested in the MTS machine.

The *S*-*N* data points (stress versus number of cycles) for different displacements obtained from fatigue tests were used to evaluate parameters such as s_0 and S_0 (goodness of fit) by regression analysis which were then inputted in the MATLAB script to fit a mathematical modified Yeoh model in ANSYS. s_0 and S_0 characterize how the materials fatigue life changes with stress, which are depicted in **Table 2**.

Table 2. Material parameters derived from the linear regression technique.

Material parameters	Displacements			
	5 mm	**10 mm**	**15 mm**	**20 mm**
s_0	0.8691	0.8974	0.9346	0.8631
S_0	2445	2035	1856	3910

3.2.3. Damage evolution using scanning electron microscope

Experimental evaluation of damage in the composite involves several methodologies tailored to assess the material's structural integrity and performance under various conditions. Scanning electron microscopy (SEM) serves as a primary tool for detailed surface analysis, offering high-resolution imaging capabilities such a s (1–10 nm) and a large depth of focus (typically 100 µm at $\times 1000$ magnification) to examine damage mechanisms such as surface damage like wear patterns and abrasions, crack formation, delamination and interface integrity [23].

The neoprene rubber samples were cut to $1\ \text{cm} \times 1\ \text{cm}$ size at the end of the gauge length of the composite specimens tested under fatigue and scanned into SEM at the resolution of 400 µm at $\times 100$ magnification to get the images for damage evaluation as shown in **Figure 5**.

(a) **(b)** **(c)**

Figure 5. SEM spectrographs after tension-tension fatigue test, **(a)** Begining of dis-integration; **(b)** Dis-integrated rubber; **(c)** Large voids in damaged rubber.

Areas of voids content present in the images were calculated in each image by image processing software for damage quantification.

Damage values shall be between 0 and 1.

$$\mathrm{D} = \frac{A_L}{A};$$

D is Damage ($0 < D < 1$), A_L is Area of void content, and A is area of specimen.

4. Theoretical analysis using matlab

In MATLAB, fatigue damage accumulation for constant amplitude histories is implemented using the principles of CDM theory. Specifically, the existing Yeoh model has been enhanced mathematically to incorporate the accumulation of damage within the elastomeric composite relative to the number of cycles endured.

The MATLAB program 1 is structured to incorporate material parameters derived from experimental uniaxial stress-strain data (C_{10}, C_{20}, C_{30}) and fatigue test data (s_0 and S_0). **Table 3** depicts all the parameters incorporated in the MATLAB script. Principal stretches I_1, I_2 and I_3 are computed based on the deformation state of the material from the deformation tensor in finite element simulations. The code is specified for the cycle counts at which the damage within the composite is to be evaluated. By inputting these cycle counts, users can obtain the damage incurred in the composite due to fatigue loading. The implementation of MATLAB in Yeoh model offers a comprehensive framework for computing fatigue damage accumulation in elastomeric composites, facilitating both experimental data and mathematical modeling to provide valuable insights into material performance under cyclic loading conditions. (see **Figure 6**)

Table 3. Parameters incorporated in MATLAB for implementation in ANSYS.

Material parameters		**Values**			
Yeoh model constants	C_{10}	0.014899			
	C_{20}	–0.00023332			
	C_{30}	0.00002187			
Materials parameters (Goodness of fit)	s_0	0.8691	0.8974	0.9346	0.8631
	S_0	2445	2035	1856	3910
Lambda = Deformed length ÷ Original length	L	1.15			
Number of cycles	N	100, 1000, 10000			

```
clear all
clc
format long
c10 = 0.014899;
c20 = -0.00023332;
c30 = 0.00002187;
S0 = 2445.0/2035.0/1856.0/3910.0;
s0 = 0.8691/0.8974/0.9346/0.8631;
a = 1 + s0;
L = 1.15; % lambda
b = (2 * L) - (2 / (L * L));
c = (L * L) + (2 / L) - 3;
d = 2 + (4 / (L * L * L));
N = [100, 1000, 10000];
term1 = ((c10 * b) + (2 * c20 * c * b) + (3 * c30 * c * c * b)) ^ 2;
term2 = (c10 * d) + (2 * c20 * (b * b + c * d));
term3 = (3 * c30) * ((2 * c * b * b) + (c * c * d));
term4 = 1 / (term2 + term3);
term5 = term1 * term4;
term6 = ((1 / S0) * term5) ^ s0;
term7 = 1 - a . * N . * term6 ;
D = 1 - (term7). ^ (1/a)
```

Figure 6. MATLAB program for modified Yeoh model.

5. Results and discussion

The comparison of damage by experimental (SEM images) and analytical analysis (MATLAB) is depicted in **Figure 7a–d** for various displacements such as 5 mm, 10 mm, 15 mm and 20 mm with corresponding damage assessment at 100, 1000 and 10,000 cycles. SEM images were exported in image processing software and damage was evaluated by measuring area of voids. A sample size of 1 cm×1cm from rubber material only in the composite specimen was cut for SEM images. Hence, damage evaluation in experimental procedure is on rubber material, whereas analytical damage analysis (MATLAB) is on the composite (rubber along with carbon fabric).

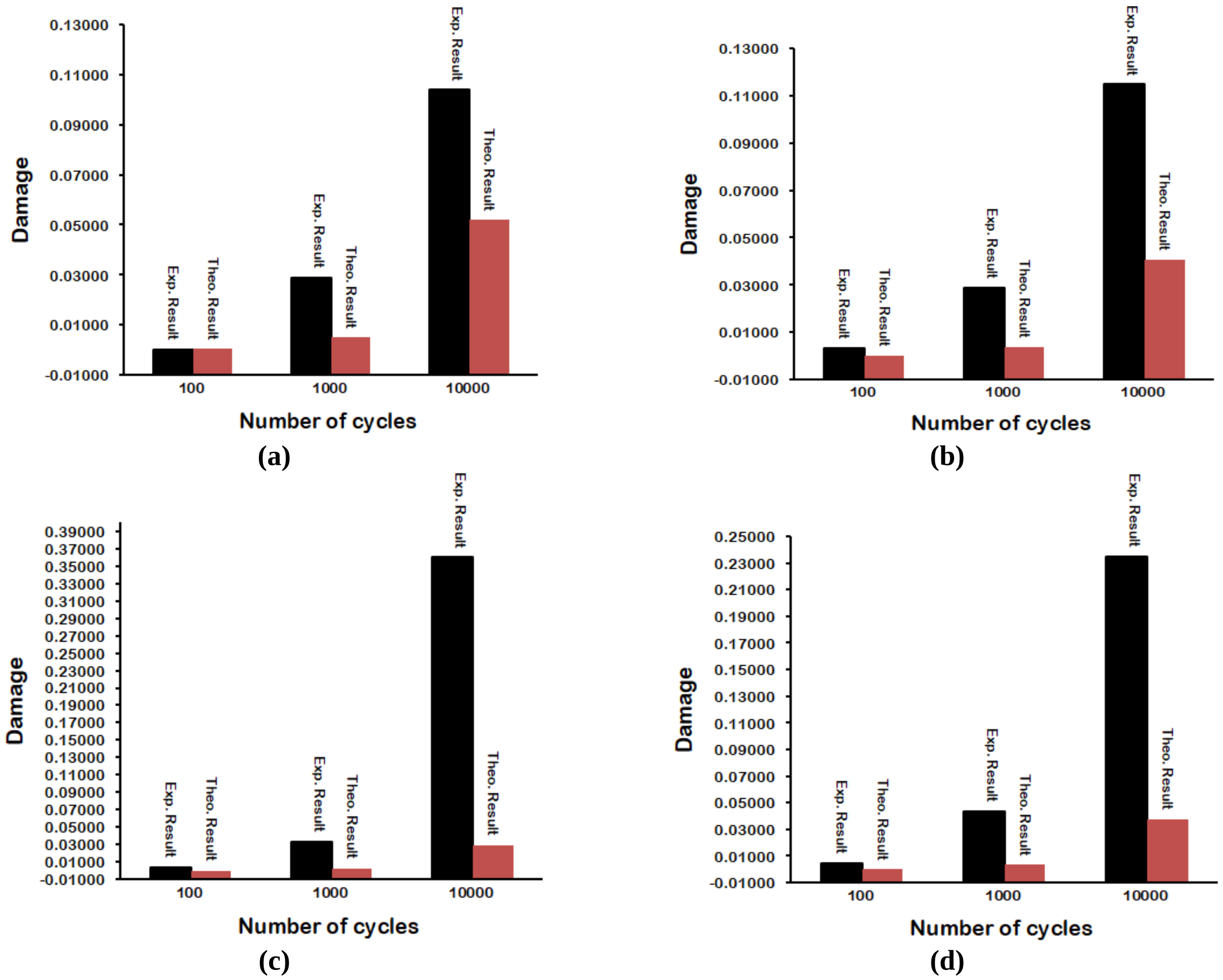

Figure 7. Comparison of damage by experimental (SEM) and analytical or theoretical (MATLAB) methods, **(a)** 5 mm displacement, where s_0 = 0.8691, S_0 = 2445; **(b)** 10 mm displacement, where s_0 = 0.8974, S_0 = 2035; **(c)** 15 mm displacement, where s_0 = 0.9346, S_0 = 1856; **(d)** 20 mm displacement, where s_0 = 0.8631, S_0 = 3910.

Experimental and analytical damage values are almost the same after 100 cycles in all four displacements. However, the difference between both damages goes on increasing with 1000 and 10,000 cycles. The same conclusion was drawn by Saman [23]. This is because of the delamination effect of neoprene rubber from the bi-directional carbon fabric. Delamination just began when specimens reached 1000 cycles, and it became substantial until 10,000 cycles were completed. Therefore, test results of 100,000 cycles are not included in the present study as the composite was delaminated completely.

Experimental damage values are significantly large because of damage to the rubber material only after delamination from the carbon fabric. Also, few specimens indicated rupture of carbon fabric in 10,000 cycles, which led to induced damage in rubber material only. The behavior and deformation of the composite is largely controlled by the carbon fabric laminate, as it is very strong and brittle in nature, whereas neoprene rubber is hyper-elastic in nature as long as there is a perfect bond between the two materials. However, the behavior of the composite is determined by neoprene rubber after debonding takes place, which is reflected in the experimental damage of the composite for 10,000 cycles in 15 mm and 20 mm displacements. Determination of effective performance of the adhesive in the composite was also the objective in this study; therefore, the composite was tested in 15 mm and 20 mm displacements under 10,000 cycles. The strength and deformation performance of any composite is determined by the effectiveness of the adhesive when two opposite natures of materials are joined together. There shall be a very effective adhesive to bond both the materials to avoid delamination, which would validate analytical damage for a higher number of cycles in fatigue.

6. Conclusions

Based on the present study, the following key conclusions are drawn regarding damage evolution from the modified Yeoh model in elastomeric composites.

a) The existing Yeoh model is employed to accurately derive the material constants in the form of mechanical properties from the experimental stress-strain response of the material in a static uniaxial tensile test. The existing mathematical framework in the Yeoh model is modified by incorporating the experimentally evaluated parameters in static and fatigue tests and then integrated using CDM principles to constitute a specialized fatigue damage model.

b) The experimental phase involves evaluation of C_{10}, C_{20} and C_{30} in axial tension specimens using a curve-fitting method in the existing Yeoh model. Also, tension-tension fatigue testing of dumbbell-shaped specimens for various displacements enables the evaluation of s_0 and S_0 by regression analysis of S-N curve. Material parameters evaluated from axial tension tests and fatigue testing are then incorporated in MATLAB scripts incorporating C_{10}, C_{20} and C_{30} values from axial tension tests and s_0 and S_0 from fatigue tests. This novel approach of achieving a damage variable for fatigue by modifying the existing Yeoh model simplified fatigue life prediction for elastomer composites.

c) The comprehensive approach of evaluating material parameters experimentally using the existing Yeoh model, mathematically modifying the existing Yeoh model for fatigue, and integrating MATLAB into the modified Yeoh model to get damage values in the composites paves the way for fatigue life prediction of elastomer composites.

d) The large difference between experimental and theoretical damage values for 10,000 cycles is owing to practical difficulties in sampling for SEM, delamination of rubber with carbon fabric, and the complex nature of deformation between two opposite natures of materials. None the less, damage prediction of the composites is promising with this modified model up to 1000 cycles for all displacements. This model is very useful to predict fatigue damage before delamination of the layers takes place.

e) The aim of this study was to integrate the experimental test results of the composite and the existing Yeoh model in order to modify the model and fit it for the prediction of the fatigue life of the composite made up of two opposite natures of materials. More rigorous study is required to take care of all the parameters involved at the interface between the two materials in the fatigue performance, that is, delamination, rupture of fibers, etc. Also, a highly effective adhesive shall be used to bond two materials in the composite to validate this simplified fatigue damage model at a higher number of cycles.

Author contributions: Conceptualization, JDR, RCS and KN; methodology, KN, SC, PC, PP, AC, JDR and RCS; software, RCS and AC; validation, JDR, RCS and AC; formal analysis, KN, SC, PC, PP, AC, JDR and RCS; investigation, KN, SC, PC, PP, AC, JDR and RCS; data curation, JDR, RCS and AC; writing—original draft preparation, KN, JDR and RCS; writing—review and editing, KN, JDR and RCS; visualization, JDR and RCS; supervision, JDR and RCS; project administration, JDR and RCS. All authors have read and agreed to the published version of the manuscript.

Acknowledgments: The authors are thankful to Reviewers and Editor for valuable comments.

Availability of data and materials: All the data related to this manuscript are included in the manuscript.

Using of AI tools: No Artificial Intelligence (AI) tools are used.

Conflict of interest: The authors declare no conflict of interest.

References

1. Le Cam JB, Huneau B, Verron E. Fatigue damage in carbon black filled natural rubber under uni- and multiaxial loading conditions. International Journal of Fatigue. 2013; 52: 82–94. doi: 10.1016/j.ijfatigue.2013.02.022
2. Kang W, Liu J, Xiong W, et al. Basic mechanical and fatigue properties of rubber materials and components for railway vehicles: A literature survey. Reviews on Advanced Materials Science. 2022; 61(1): 587–610. doi: 10.1515/rams-2022-0054
3. Suryatal B, Phakatkar H, Rajkumar K, et al. Fatigue Life Estimation of an Elastomeric Pad by ε-N Curve and FEA. Journal of Surface Engineered Materials and Advanced Technology. 2015; 05(02): 85–92. doi: 10.4236/jsemat.2015.52010
4. Yeoh OH. Hyperelastic material models for finite element analysis of rubber. Journal of Natural Rubber Research. 1997; 12(3): 142–153.
5. Ali A, Hosseini M, Sahari B. Continuum damage mechanics modeling for fatigue life of elastomeric materials. International Journal of Structural Integrity. 2010; 1(1): 63–72. doi: 10.1108/17579861011023801
6. Zarrin-Ghalami T, Fatemi A. Cumulative fatigue damage and life prediction of elastomeric components. Fatigue & Fracture of Engineering Materials & Structures. 2012; 36(3): 270–279. doi: 10.1111/j.1460-2695.2012.01720.x
7. Tang CY, Lee WB. Damage mechanics applied to elastic properties of polymers. Engineering Fracture Mechanics. 1995; 52(4): 717–729. doi: 10.1016/0013-7944(94)00333-D
8. Mars WV, Fatemi A. A literature survey on fatigue analysis approaches for rubber, International Journal of Fatigue. 2002; 24(9): 949–961. doi: 10.1016/S0142-1123(02)00008-7

9. Barbero EJ, Shahbazi M. Determination of material properties for ANSYS progressive damage analysis of laminated composites. Composite Structures. 2017; 176: 768–779. doi: 10.1016/j.compstruct.2017.05.074
10. Shangguan WB. Study on the Effect of Different Damage Parameters on the Predicting Fatigue Life of Rubber Isolators. Journal of Mechanical Engineering. 2016; 52(2): 116-126. doi: 10.3901/jme.2016.02.116
11. Shangguan WB, Wang XL, Deng JX, et al. Experiment and modeling of uniaxial tension fatigue performances for filled natural rubbers. Materials & Design. 2014; 58: 65–73. doi: 10.1016/j.matdes.2014.01.035
12. Gehrmann O, Kröger NH, Muhr A. Displacement-controlled fatigue testing of rubber is not strain-controlled. International Journal of Fatigue. 2021; 145: 106083. doi: 10.1016/j.ijfatigue.2020.106083
13. Luo RK. Rubber fatigue prediction for filled natural rubber under positive and negative R ratios. International Journal of Fatigue. 2022; 158: 106769. doi: 10.1016/j.ijfatigue.2022.106769
14. Wang X, Shangguan W, Rakheja S, et al. A method to develop a unified fatigue life prediction model for filled natural rubbers under uniaxial loads. Fatigue & Fracture of Engineering Materials & Structures. 2014; 37(1): 50–61. doi: 10.1111/ffe.12081
15. Li Q, Zhao J, Zhao B. Fatigue life prediction of a rubber mount based on test of material properties and finite element analysis. Engineering Failure Analysis. 2009; 16(7): 2304–2310. doi: 10.1016/j.engfailanal.2009.03.008
16. Papadopoulos IC, Thomas AG, Busfield JJC. Rate transitions in the fatigue crack growth of elastomers. Journal of Applied Polymer Science. 2008; 109(3): 1900–1910. doi: 10.1002/app.28086
17. Ayoub G, Naït-abdelaziz M, Zaïri F, et al. Multiaxial fatigue life prediction of rubber-like materials using the continuum damage mechanics approach. Procedia Engineering. 2010; 2(1): 985–993. doi: 10.1016/j.proeng.2010.03.107
18. Wang B, Lu H, Kim GH. A damage model for the fatigue life of elastomeric materials. Mechanics of Materials. 2002; 34(8): 475-483. doi: 10.1016/S0167-6636(02)00175-8
19. Lemaitre J. A Continuous Damage Mechanics Model for Ductile Fracture. Journal of Engineering Materials and Technology. 1985; 107(1): 83–89. doi: 10.1115/1.3225775
20. Pamar JD, Naik BB, Latha OH, et al. Experimental Investigation of Bi Directional Carbon Fiber Composite. Materials Today: Proceedings. 2015; 2(4–5): 3008–3016. doi: 10.1016/j.matpr.2015.07.285
21. ASTM, D3039/D3039M. Standard test method for tensile properties of polymer matrix composite materials. ASTM International. 2002.
22. D412-98aASTM. Standard test methods for vulcanized rubber and thermoplastic elastomers. Annual Book of ASTM Standards; 2003.
23. Saman F. Void content computation using optical microscopy for carbon fiber composites, Degree project in the field of technology materials design and engineering and the main field of study materials science and engineering. Stockholm Sweden; 2020.